What Dense Graph Do You Need for Self-Attention?

Yuxing Wang [1 2] **Chu-Tak Lee** [1] **Qipeng Guo** [1] **Zhangyue Yin** [1] **Yunhua Zhou** [1]
Xuanjing Huang [1 2] **Xipeng Qiu** [1 3]

Abstract

Transformers have made progress in miscellaneous tasks, but suffer from quadratic computational and memory complexities. Recent works propose sparse Transformers with attention on sparse graphs to reduce complexity and remain strong performance. While effective, the crucial parts of how dense a graph needs to be to perform well are not fully explored. In this paper, we propose Normalized Information Payload (NIP), a graph scoring function measuring information transfer on graph, which provides an analysis tool for trade-offs between performance and complexity. Guided by this theoretical analysis, we present Hypercube Transformer, a sparse Transformer that models token interactions in a hypercube and shows comparable or even better results with vanilla Transformer while yielding $O(N \log N)$ complexity with sequence length N. Experiments on tasks requiring various sequence lengths lay validation for our graph function well[1].

1. Introduction

In recent years, self-attention and its implementation Transformers (Vaswani et al., 2017) have achieved great success in a wide variety of Natural Language Processing (NLP) (Devlin et al., 2019; Vaswani et al., 2017; Miller, 2019; Sun et al., 2019) and Computer Vision (CV) (Yuan et al., 2021; Dosovitskiy et al., 2021) tasks.

The key innovation of self-attention mechanism is to allow each token to interact with others directly, and thus avoid the long-term dependency problem. However, this results in the quadratic computational and memory complexity with the sequence length. To improve model efficiency, many lightweight Transformers are proposed (Tay et al., 2020b; Lin et al., 2021). Among them, sparse Transformers (Zaheer et al., 2021; Beltagy et al., 2020; Child et al., 2019; Guo et al., 2019) utilize sparse attention in the self-attention mechanism including global attention, window attention or rule-based sparse attention.

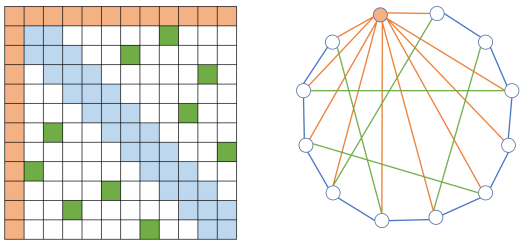

Figure 1. Attention map and its corresponding graph.

Previous works view sparse attention as self-attention on sparse graphs. Figure 1 shows typical sparse attention map and its corresponding graph. Vanilla self-attention can be regarded as a complete graph. Although these Sparse Transformers have made progress, there still remains some questions: which property is important for those graphs serving as ground for self-attention? How dense do we need the graph to be in order to reduce complexity and at the same time remain performance? While some (Zaheer et al., 2021; Chen et al., 2021) showed theoretical analysis for existing sparse self-attention, they do not provide a general analysis tool for comparing different sparse patterns.

To investigate further into differences between sparse patterns, we need theoretical analysis based on sparse graphs. In this paper, we propose Normalized Information Payload (NIP), a graph scoring function to measure information transfer on a given graph. Our function can also be applied to analyze previous sparse patterns and provide insights for their empirical results. Guided with our proposed function, we further present Hypercube Transformer which adapts hypercube into self-attention and achieves great balance between performance and computation costs. Experiments in long-context sequence modeling and large-corpus pretrain-

[1]School of Computer Science, Fudan University [2]Institute of Modern Languages and Linguistics, Fudan University [3]Peng Cheng Laboratory. Correspondence to: Yuxin Wang <wangyuxin21@m.fudan.edu.cn>, Xipeng Qiu <xpqiu@fudan.edu.cn>.

Proceedings of the 39^{th} International Conference on Machine Learning, Baltimore, Maryland, USA, PMLR 162, 2022.

[1]Code is available at https://github.com/yxzwang/Normalized-Information-Payload.

ing show that Hypercube Transformer is competitive both theoretically and practically.

The contributions of our paper can be summarized as follows:

- We propose Normalized Information Payload (NIP), a graph scoring function that tries to investigate important properties of graph used in self-attention. This function provides theoretical analysis tools for performance and complexity of different graphs used in position-based sparse self-attention.
- Guided with our theoretical analysis, we present Hypercube Transformer, which can behave competitively compared to vanilla Transformer in various tasks and better in long context tasks while requiring less time and computation.

2. Graph Scoring Function for Balancing Costs and Performance

What Dense Graph Do We Need? Self-attention (vanilla and sparse) can be viewed as attention-based information transfer on graphs. While many sparse patterns based on sparse graphs have been presented, there still remains questions: what is important for a sparse graph in self-attention? What dense graph do we need for self-attention? How dense is optimal for the graph to balance cost and performance? To answer these questions, we propose Normalized Information Payload, a graph scoring function to score any graphs used for self-attention.

2.1. Normalized Information Payload

Generally, we expect our model to grab all interactions among tokens. Sparse attentions indirectly capture these interactions by multi-layer information transfer. That comes to two questions: what costs do we pay for grabbing these interactions and how much information can be transferred? To answer these questions respectively, we consider graphs in two aspects: Computational Complexity and Information Payload.

Computational Complexity. Computational Complexity (CC) of a graph G, denoted by $\mathrm{CC}(G)$, is the computation complexity required to allow the model to grab all interactions among tokens when using graph G for self-attention. The requirement for graph G used here is that G is connected. Lower Computational Complexity of a graph makes the whole model less computational expensive.

Information Payload. The amount of information transfer is also important. For instance, sequence models like LSTMs (Hochreiter & Schmidhuber, 1997) is able to transfer information in a long sequence but suffers from long-term dependency and low information capacity. So we introduce Information Payload (IP) for a graph G, denoted by $\mathrm{IP}(G)$, measuring how much information a graph can transfer when allowing the model to grab all interactions among tokens. Higher Information Payload of a graph enables the whole model to grab more information.

To better compare information transfer on different graphs, we define the Normalized Information Payload for a graph G, denoted by $\mathrm{NIP}(G)$, as follows,

$$\mathrm{NIP}(G) := \frac{\mathrm{IP}(G)}{\mathrm{CC}(G)}. \tag{1}$$

The higher $\mathrm{IP}(G)$ is, the more information a graph can transfer. The lower $\mathrm{CC}(G)$ is, the less computational resources the graph costs, which also means that the graph can be used to model long sequences. And the higher score of $\mathrm{NIP}(G)$ implies the graph can perform well in real-world tasks. This is consistent with our observations in experiments. Then we will demonstrate how these two components of our function are defined in detail and show how previous works like BigBird fit our function. For a self-attention layer on graph G, we denote it by G-attention layer briefly.

2.1.1. Computational Complexity

Computational Complexity is related to grabbing all interactions among tokens. Given a G-attention layer, to make the whole model grab all interactions among tokens, we need to stack $\kappa(G)$ G-attention layers. Straightforwardly, $\kappa(G)$ is the diameter of graph G. And for one G-attention layer, the Computational Complexity is proportional to the total number of edges in G. When the input sequence is fixed at length N, the Computational Complexity for one layer is proportional to the mean degree of G, which we denoted by $\rho(G)$ here. Intuitively $\rho(G)$ measures the complexity of the graph itself and $\kappa(G)$ is how many times we forward the graph.

Definition 2.1. Let Computational Complexity CC for a given graph G be

$$\mathrm{CC}(G) := \rho(G) \times \kappa(G). \tag{2}$$

$\mathrm{CC}(G)$ shows the minimum computation costs to ensure information exchange for every node pair in a graph.

2.1.2. Information Payload

To capture all interactions among tokens is not enough, we have to take into account how much information a graph can transfer after that. Information Payload is introduced to measure it. First we examine how information transfer is like in self-attention. Since we have Softmax operation in self-attention mechanism acting as normalization, it is straightforward to set the total amount of information a

Table 1. Normalized Information Payload for commonly used graphs, where w is the number of neighbors in ring lattice. $\star$: $\Theta\left(\frac{1}{N^2}\right)$ after refinement.

Type of graph	CC(G) ↓	IP(G) ↑	NIP(G) ↑
Complete	$\Theta(N)$	$\Theta\left(\frac{1}{N}\right)$	$\Theta\left(\frac{1}{N^2}\right)$
E-R random	$\Theta(\log^2 N)$	$\Theta\left(\frac{(N-2)!}{N^{\log N}(N-\log N)!}\right)$	$\Theta\left(\frac{(N-2)!/(N-\log N)!}{N^{\log N}\log^2(N)}\right)$
Tree	$\Theta(\log N)$	$\Theta(\frac{1}{N^{\log(9)}})$	$\Theta\left(\frac{1}{N^{\log(9)}\log N}\right)$
Star	$\Theta(1)$	$\Theta\left(\frac{1}{N}\right)$	$\Theta\left(\frac{1}{N}\right)^\star$
Ring lattice + E-R random	$\Theta(\log N(\log N + w))$	$\Theta\left(\frac{(N-2)!}{(N+\frac{w}{\log N})^{\log N}(N-\log N)!}\right)$	$\Theta\left(\frac{(N-2)!/(N-\log N)!}{(N+\frac{w}{\log N})^{\log N}\log N(\log N+w)}\right)$
Ring lattice + Star (Longformer)	$\Theta(w)$	$\Theta\left(\frac{1}{Nw}\right)$	$\Theta\left(\frac{1}{Nw^2}\right)$
Ring lattice + Star + E-R random (BigBird)	$\Theta(\log N + w)$	$\Theta\left(\frac{1}{N(\log N+w)}\right)$	$\Theta\left(\frac{1}{N(\log N+w)^2}\right)$
Hypercube	$\Theta(\log^2 N)$	$\Theta\left(\frac{(\log N)!}{(\log N)^{\log N}}\right)$	$\Theta\left(\frac{(\log N)!}{(\log N)^{\log N+2}}\right)$

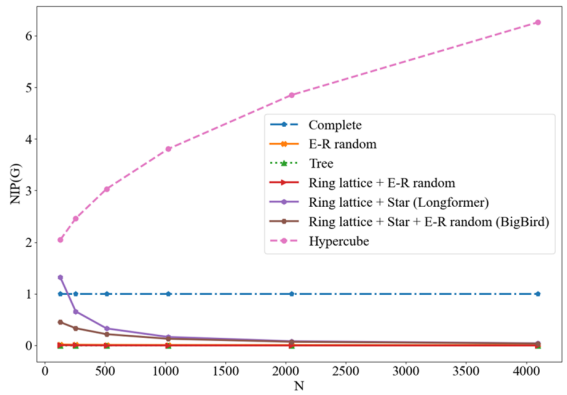

Figure 2. NIP(G) for graphs divided by complete graph in Table 1. We do not include star graph and ring lattice in this Figure because NIP(G) for star graph is too large. The w used for ring lattice is set to $\frac{N}{16}$ according to Longformer at length 4096.

node can receive as one unit of information. For one node i with degree $deg(i)$, the average information it can receive is $\frac{1}{deg(i)}$, so the total Information Payload for one path is related to all end nodes on the path.

Notation. Given a graph $G(\mathcal{V}, \mathcal{E})$, and nodes a, b, let $\mathcal{P}_{ab}$ be the set of all paths that start with node a and end with node b and have length equal to the distance between node a and node b. For one path $P_{ab} \in \mathcal{P}_{ab}$, $len(P_{ab})$ is the length of P_{ab}. For one node i, we use $deg(i)$ to denote the degree of it.

Definition 2.2. For one path $P_{ab} \in \mathcal{P}_{ab}$, the Information Payload of one path P_{ab}, denoted by $R(P_{ab})$, is defined as

$$R(P_{ab}) := \prod_{v \in P_{ab} \ \& \ v \neq a} \frac{1}{deg(v)}. \tag{3}$$

Next we define the Information Payload between node a and node b.

Definition 2.3. The Information Payload between node pair (a, b), denoted by I_{ab} is sum of Information Payload of all paths that belong to $\mathcal{P}_{ab}$:

$$I_{ab} = \sum_{P_{ab} \in \mathcal{P}_{ab}} R(P_{ab}). \tag{4}$$

Note that $\frac{1}{k_i}$ is equal to the probability that a random walk starts from the node itself to any of its neighbors, which makes our Information Payload closely related to random walk on graphs.

Relationship between Information Payload and Random Walk. Our Information Payload is deduced from self-attention forward, which is closely related to random walk. We show in Figure 3 that self-attention is like reversed random walk. In Figure 3, each column shows a G-attention layer and we have t layers. For G used here, we present three nodes a, b, c and edges (a, b), (a, c) and self-loop of three nodes. Figure 3(a) shows the updating of G-attention layers. The red paths show the information transferred from node a to node c. In Figure 3(b), blue paths show the random walk starts from node c to node a. We can see that the Information Payload from node a to node c after t layers is equal to the probability of a random walk starting from node c ends in node a at the tth step. We demonstrate it in the theorem below in detail.

Theorem 2.4. *Information Payload between two nodes I_{ab} equals to the probability of a random walk starts from node b that ends in node a at step $len(P_{ab})$.*

Proof of theorem 2.4 and calculating I_{ab} via random walk is in Appendix B.1.

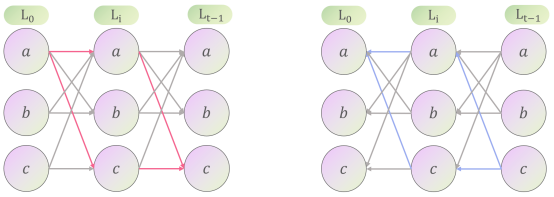

(a) Attention forward (b) Random walk

Figure 3. Relationship between G-attention layer and random walk. Red lines in Figure (a) shows attention forward from node a to node c across t layers while blue lines in Figure (b) shows random walk starting from node c to node a.

Note that the probability of a random walk starts from b that ends in a within $len(P_{ab})$ steps equals to zero. Thus I_{ab} measures the amount of information when information flow first reaches node a from node b.

Since we have defined the Information Payload between two nodes, the Information Payload for the whole graph is chosen to the Information Payload between node pairs (a, b) whose distance is the diameter of the graph.

Definition 2.5. The Information Payload for a graph G $\text{IP}(G)$ is the smallest Information Payload I_{ab} between node pairs (a, b) whose distance is the diameter of the graph. Let Δ be the set of node pairs whose distance is the diameter of the graph, we have

$$\text{IP}(G) := \min_{(a,b)\in\Delta} I_{ab}. \tag{5}$$

We consider the minimum Information Payload for node pair (a, b) whose distance is the diameter, so we choose the smallest value to guarantee the lower bound of Information Payload, which is motivated by the theory of the Cannikin Law (Li et al., 2019), that the capacity of the wooden bucket is limited by the height of its shortest plank.

2.1.3. Discussion

Table 1 lists $\text{CC}(G)$, $\text{IP}(G)$ and $\text{NIP}(G)$ for commonly used graphs[2]. The detailed computation is in Appendix A.

Self-loop. In self-attention, a token can always attend to itself, meaning that all graphs have self-loop. $\text{IP}(G)$ use node pair whose distance is the diameter of the graph, so self-loop does not affect its value much. Also $\text{CC}(G)$ does not change much even if we have a large number of nodes. Thus $\text{NIP}(G)$ does not change much compared to graphs without self-loop.

Markov Chains. In self-attention, the information updating for a node is not uniform with its neighbors but dependent on representations of all relative nodes, which is not the case of normal random walk. However, previous analysis (Clark et al., 2019) on BERT attention shows that some attention heads, especially in lower layers, have very **broad attention**. Since information in lower layers is closer to the input and is important, we set the uniform distribution of attention weights and this setting is also the situation of random initialization. Also, viewing random walk as Markov chains can bring insights into this situation. If we let the transition matrix in Markov chains be attention-based, then normal random walk becomes attention-based random walk, which is suitable for self-attention.

[2]In this paper, all log means $\log_2$.

2.2. Case study

To make $\text{NIP}(G)$ clear, we show in Figure 2 all the $\text{NIP}(G)$ in Table 1 except star graph. Because $\text{NIP}(G)$ for star graph is too large.

Star graph.

Star graph has the highest $\text{NIP}(G)$, however, huge amounts of information flow through the global node can cause a bottleneck of information transfer. This bottleneck reduces the Information Payload of star graph to $\frac{1}{N-1}$ of the original one because $N-1$ local nodes versus one global node. Thus, the refined $\text{NIP}(G)$ of star graph is $\Theta\left(\frac{1}{N^2}\right)$.

Ring lattice. Ring lattice is often used in self-attention known as window attention or local attention. It is usually combined with other attention patterns so we compute NIP for its mixtures. Most of attention occupies in neighborhoods (Cui et al., 2019), which makes previous sparse patterns adapting it reasonable.

Random graphs. We compute the expected values for random graphs in this paper. For the Erdős–Rényi (E-R) random graph used in BigBird, if the probability of every edge to exist is p, the E-R random graph is highly possibly connected if $p > \frac{(1+\epsilon)\ln(N)}{N}$. This means that to make connected random graphs with high probability, the average degree of the graph is more than $\frac{(1+\epsilon)\ln(N)(N-1)}{2N}$. We use the lower bound and set p to $\Theta\left(\frac{\log N}{N}\right)$ here. We limit the choice of random graphs in this paper to E-R random graph because it has been applied in self-attention.

BigBird, Longformer and mixed graphs. BigBird is mixed from star graph, ring lattice and random graph, while Longformer is only mixed from star graph and ring lattice. For BigBird, because of random graph, we compute the expected $\text{NIP}(G)$ for a given graph G. We use the settings for random graph as we mentioned in above paragraph. We have shown that adding random graph to Longformer like BigBird not necessarily improves the Normalized Information Payload for the graph because it makes the graph more complex and reduces the expectation Information Payload. While such observation is counterintuitive, the BigBird-ETC

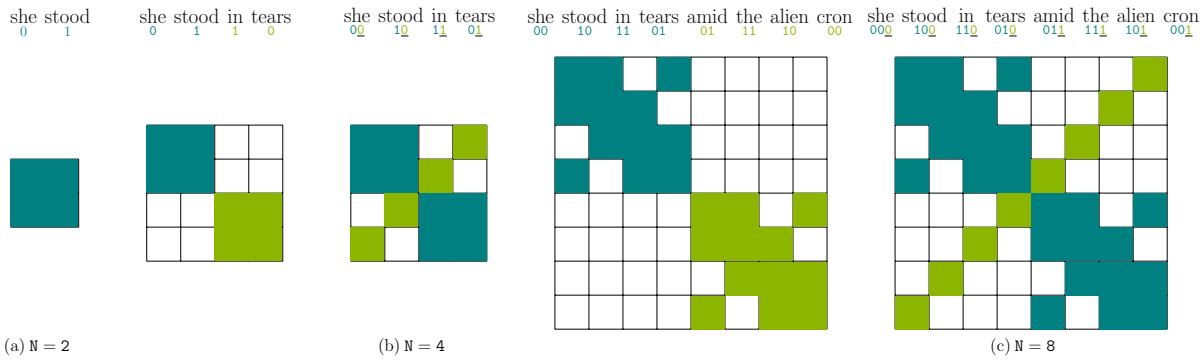

Figure 4. Iteratively mapping a sequence to a hypercube and its attention mask. Figure (a), (b) and (c) is the attention map for input sequences with length $N = 2, 4, 8$ respectively.

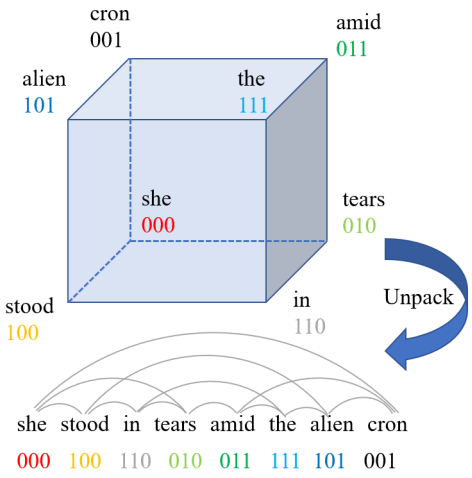

Figure 5. Unpacking a hypercube to a sequence. Tokens that are neighbors in hypercube are also neighbors in a sequence.

which is sota in BigBird models also despose random attention. Our ablation studies in the experiment section (in Table 2) also demonstrate that mixing Longformer with random attention does not necessarily improve the performance.

3. Hypercube Transformer

Guided with our Normalized Information Payload, we aim to find better graphs for self-attention and present Hypercube Transformer. Like vanilla Transformer, our Hypercube Transformer utilize positional embeddings to catch positional information.

3.1. Hypercube

The global node in star graph is very important but suffers from information interference as mentioned before. Hence we search for regular graphs with no inductive bias to alleviate information interference. An observation for complete graph is that the shortest distance between two neighbors' neighbors (excluding two nodes themselves) equals to zero, meaning that every two neighbor has the same neighbor. We propose a graph in which this distance equals to one, which makes the whole graph much sparser while maintaining the connectivity of the graph, and that graph is hypercube.

After our computation, hypercube is potential according to our Normalized Information Payload. It has Normalized Information Payload larger than other sparse graphs except star graph as shown in Figure 2. At the same time, small $\mathrm{CC}(G)$ means hypercube can be applied to long sequences. Also, in parallel computing, hypercube is one of the most useful communication structures which encounters not much communication interference.

3.2. Mapping Sequences to Hypercube[3]

Although we show that hypercube is potential in Normalized Information Payload, it's hard to apply it to real-world tasks if we can't map sequences to hypercube. Generally, we suggest a mapping method have two good properties:maintaining the original neighborhoods in sequences and easy to be extended to longer sequences. One example of unpacking hypercube to sequence is shown in Figure 5. Here we propose a novel iterative binary-number-based mapping from sequence to hypercube. We show this iterative binary mapping algorithm in Appendix B.3. We also show the iterative mapping pipeline and its attention map in Figure 4.

If the dimension of binary numbers is k, the final binary representation for token with index i ($X_i :=$

[3]We thank Anjiang Wei at Stanford University for his help.

$X_i^{k-1}X_i^{k-2}...X_i^1X_i^0, i \in [0, N-1]$) is given by

$$X_i^d = \left(\lfloor \frac{i \mod 2^{k-d+1}}{2^{k-d}} \rfloor + \lfloor \frac{i \mod 2^{k-d}}{2^{k-d-1}} \rfloor \right) \mod 2, \tag{6}$$

where $\lfloor x \rfloor$ means the largest integer smaller than x. We denote the set of representation that has only one digit different from X_i by $\mathcal{N}(X_i)$. After we got X_i for every token with index i, we can easily draw the attention map by the rule that one token with representation X_i can only attend to tokens with representation $X_j \in \mathcal{N}(X_i)$.

3.3. Block Sparsity

Block sparse pattern is introduced by (Gray et al., 2017) to tackle hardware problems for efficient calculating. It splits the sequence into several blocks and impose sparse patterns on blocks instead of tokens. Tokens can attend to every token in the same block and the block its block can attend to. Adapting block sparse lowers the sparsity of graph and intensifies information passing when the number of G-attention layer is fixed. While all sparse patterns adapt block sparse, we don't compare those patterns after adapting block sparse. However, we consider how block sparse have effects on sparse patterns and we have the theorem below.

Theorem 3.1. *For block size $b \leq \frac{N}{2}$, larger block size makes star graph and hypercube have less Normalized Information Payload.*

We put the proof in Appendix B.2. Although block sparse reduces Normalized Information Payload in most situation, we still adapt it in our experiment section for the sake of training efficiency.

4. Experiments

Experiments are conducted to validate theoretical results of Normalized Information Payload and then show performances of Hypercube Transformer. All experiments are conducted on RTX 3090 GPU. In detail, We implement all Sparse Transformers with self-loop and block sparse using triton (Tillet et al., 2019). We choose to conduct experiments mainly on block size 16 which is the smallest size allowed for triton. Recent work (Guo et al., 2021) also shows that block size 16 is cost effective on long range text tasks.

4.1. NIP(G) and Performance on LRA

To validate Normalized Information Payload, we focus on how our Normalized Information Payload is related to real-world situations. We rely on Long Range Arena (LRA) benchmark (Tay et al., 2020a) for validation for our graph scoring function, NIP(G). Long Range Arena is a benchmark testing how well a model can capture long range dependencies with tasks with input lengths varied from 1024 to 4096. By deliberately making the task harder, such as training text on byte level and image on pixel level, LRA serves as a systematic and popular proxy for performance to computational efficiency. In our case, LRA restricts models to have equal or less than four layers, making it a good test bed for layer efficiency. We choose several different graphs and apply them on G-attention layers in Transformer to evaluate performance.

Implementation details. For the sake of consistency and simplicity, we do not strictly follow setting in the official implementation. Instead we use a four-layer network, in which every two layers with shared parameters for all tasks. All hyper-parameters are listed in Table 9 in Appendix C. Empirically we find that our architecture has fewer parameters than the original paper. We follow optimization configuration in (Ma et al., 2021) and run experiments for different sparse graphs listed in Table 1. Results for our experiments and Normalized Information Payload according to Table 1 with $N = 2048$ are in Table 2. We run each experiment for three times with different random seeds and report the average accuracy.

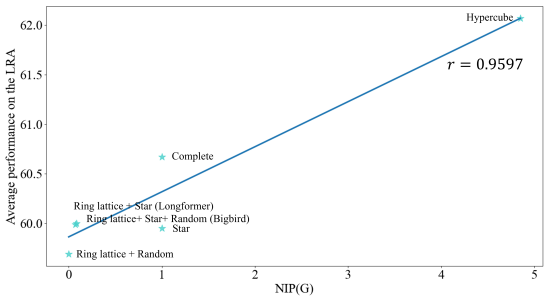

Figure 6. Average performance on the LRA benchmark can have strong proposition with our proposed Normalized Information Payload.

Results. In Table 2, we observe that Hypercube Transformer outperforms all other graphs including complete graph in average. Apart from star graph, which suffers from information interference in the global node and results in learning problems, other graphs' performance fits Normalized Information Payload well. We draw the average performance of various graphs on the LRA benchmark to NIP(G) in Figure 6 for these graphs. The average performance is strongly proportional to Normalized Information Payload in that the Pearson Correlation Coefficient between two variables is equal to **0.96**, which lays validation for our graph scoring function well.

Speedup. For speedup, we only report the training speedup of hypercube compared to complete graph at 4096 length. We do not compare hypercube with other sparse patterns

Table 2. Performances for different graphs on Long-Range Arena. $\star$ means after refinement.

Graph #Length	**ListOps** 2K	**Text** 4K	**Retrieval** 4K	**Image** 1K	**Pathfinder** 1K	**Avg.**	**NIP**(G)	**SpeedUp**
Complete	37.20	63.54	81.00	47.23	**74.39**	60.67	$1\times$	$1\times$
Star	37.58	63.37	79.71	52.19	66.92	59.95	$1\times^{\star}$	-
Ring lattice + E-R random	36.44	**63.81**	80.17	50.88	67.14	59.69	$1.43e^{-10}\times$	-
Ring lattice + Star (Longformer)	37.55	61.12	80.53	52.13	68.66	60.00	$8.25e^{-2}\times$	-
Ring lattice + Star + E-R random (BigBird)	**37.80**	62.34	79.49	52.87	67.44	59.99	$7.21e^{-2}\times$	-
Hypercube	37.48	63.79	**81.16**	**53.79**	74.12	**62.07**	$4.85\times$	$15.8\times$

because to make fair comparison between BigBird pattern and hypercube, we choose the number of blocks for each pattern to be the same. Therefore, the speedup of two sparse patterns are close. Detailed block numbers are listed in Appendix C.

Table 3. Performance of Hypercube Transformer with different block sizes.

Hypercube	**Retrieval**	**Image**
Block size 16	81.16	53.79
Block size 32	80.74	51.98
Block size 64	80.75	50.75

Block size impact. From Table 2, we find that Retrieval and Image can differentiate graphs better among five sub-tasks. So to validate theory 3.1, we investigate how block size affects performance empirically on these two sub-tasks of LRA. In Table 3, we find that larger the block size, lower the performance is, which is corresponding to our theory 3.1 that larger block size will result in lower Normalized Information Payload.

4.2. Long-Context Sequence Modeling

To show the effectiveness of Hypercube Transformer, we present the performances of previous works on LRA briefly in Table 4. Compared to recent Fnet (Lee-Thorp et al., 2021), Nystromformer (Xiong et al., 2021), LUNA (Ma et al., 2021), H-Transformer-1D (Zhu & Soricut, 2021), Pixelfly (Chen et al., 2021), our Hypercube Transformer achieves better average performance while using architecture with fewer parameters. H-Transformer-1D has very good performance on NLP tasks because their hierarchical method provides inductive bias for natural language. Hypercube Transformer improves the result of Image by a large margin because hypercube is like high-dimensional view of a picture and can catch more information. In summary, Hypercube Transformer shows potential for models only based on sparse graphs that can grab all interactions among tokens.

Table 4. Performances for different models on Long Range Arena. The performance of previous works in the first area are from (Tay et al., 2020a).

Model #Length	**ListOps** 2K	**Text** 4K	**Retrieval** 4K	**Image** 1K	**Path.** 1K	**Avg.**
Transformer	36.37	64.27	57.46	42.44	71.40	54.39
Local Attention	15.82	52.98	53.39	41.46	66.63	46.06
Sparse Trans.	17.07	63.58	59.59	44.24	71.71	51.24
Longformer	35.63	62.85	56.89	42.22	69.71	53.46
Linformer	35.70	53.94	52.27	38.56	76.34	51.36
Reformer	37.27	56.10	53.40	38.07	68.50	50.67
Sinkhorn Trans.	33.67	61.20	53.83	41.23	67.45	51.39
Synthesizer	36.99	61.68	54.67	41.61	69.45	52.88
BigBird	36.05	64.02	59.29	40.83	74.87	55.01
Linear Trans.	16.13	65.90	53.09	42.34	75.30	50.55
Performer	18.01	65.40	53.82	42.77	77.05	51.41
Fnet	35.33	65.11	59.61	38.67	77.80	55.30
H-Trans.-1D	**49.53**	**78.69**	63.99	46.05	68.78	61.41
Nystromformer	37.15	65.52	79.56	41.58	70.94	58.95
Luna-256	37.98	65.78	79.56	47.86	**78.55**	61.95
Pixelfly	37.65	66.78	80.55	42.35	72.01	59.86
Hypercube Trans.	37.48	63.79	**81.16**	**53.79**	74.12	**62.07**

4.3. Masked Language Modeling for Large-Scale Pretraining

One important application of Transformer is Large-Scale Pretraining like BERT (Devlin et al., 2019). Here we follow (Devlin et al., 2019; Izsak et al., 2021) to pretrain Hypercube Transformer from scratch, denoted by CubeBERT, and finetune it on downstream tasks. We denote the original BERT-large by BERT, our pretrained BERT-large with 128 length by BERT_{128}, and our pretrained CubeBERT-large with 128 length by CubeBERT_{128}. The detailed structure of CubeBERT is the same as BERT and experimental details are provided in Appendix C. We use English Wikipedia and BookCorpus2 (Gao et al., 2020) as our pretraining datesets.

Finetuning on longer contexts. We first finetune BERT_{128} and CubeBERT_{128} on a language model dataset Wikitext103 that could model sequences at 512 length to show the strong

Table 5. Finetuning MLM on Wikitext103.

Model	Loss	Speedup
BERT_{128}	1.18	1×
CubeBERT_{128}	1.05	1.4×

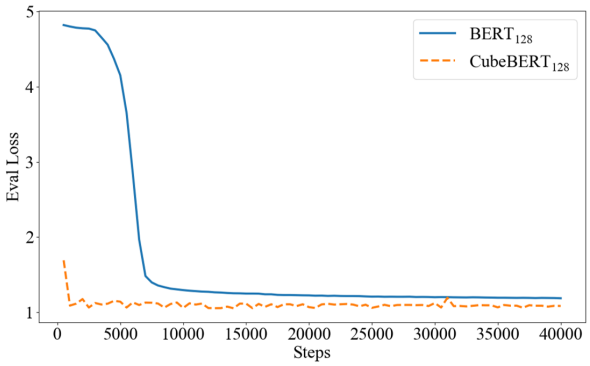

Figure 7. CubeBERT_{128} shows faster dropping rate of eval loss than BERT_{128} when finetuning on Wikitext103.

generalization ability of Hypercube Transformer. We initiate the position embeddings out of 128 randomly and finetune BERT_{128} and CubeBERT_{128} in a Masked Language Model (MLM) way, results are provided in Table 5. We can see that the MLM loss (perplexity) of finetuned CubeBERT_{128} (1.05) is lower than that (1.18) of our BERT_{128}, demonstrating the better generalization ability of Hypercube Transformer than vanilla one. At the same time, attribute to sparse attention, CubeBERT_{128} still has a 1.4x speedup compared to BERT_{128} at the training stage of finetuning. Another interesting finding is that the evaluation loss of CubeBERT_{128} drops faster than BERT_{128}, implying that Hypercube Transformer could learn faster for training short and finetuning long in certain circumstances.

Finetuning on GLUE. For downstream tasks at 128 length, we finetune CubeBERT_{128} on GLUE benchmark and compare CubeBERT_{128} with BERT. Results are reported in Table 6. To do fair comparison, we also provide finetuning results for our reimplemented BERT_{128}. We observe that CubeBERT_{128} achieves comparable performance without global attention routing information directly to [CLS] token. This demonstrate Hypercube sparsity is effective on information passing on graph. In detail, our CubeBERT_{128} can have on par performance with BERT in most tasks (MNLI, QQP, SST-2, CoLA, STS-B), all with differences less than 1 point. For rest tasks like QNLI, RTE and MRPC, CubeBERT_{128} is lower than BERT in 2 points except MRPC which has the smallest number of dataset examples. Overall, the average performance of CubeBERT_{128} is slightly lower than BERT within 1 point and higher than BERT_{128}. The speedup for CubeBERT_{128} is measured at the training training for finetuning GLUE. Because of the sequence length is 128, speedup is 1.1x, which is not remarkable compared to 1.4x for sequence at 512 length.

5. Related Work

To the best of our knowledge, our paper is related to sparse attention and their analysis.

Theoretical Analysis. Previous works mainly focus on the approximation of sparse attention to vanilla attention. BigBird (Zaheer et al., 2021) first proved sparse attention mechanism defined by any graph containing star graph is a universal approximator. They also showed Turing Completeness of sparse encoder and sparse decoder. Pixelated Butterfly (Chen et al., 2021) proved their flat butterfly matrices can approximate butterfly matrices which can tightly represent all structured matrices. Our paper focuses on finding graphs with better properties, not graphs to approximate complete graph. Axial Attention (Ho et al., 2019) mentioned having the full receptive field, which is similar to grabbing all interactions among tokens in the paper. (Li et al., 2019) proposed Information Capacity between two nodes based on the path transferring least information while we propose Information Payload based on all paths between two nodes.

Sparse Attention. Previous Transformers adapt sparse attention including Star Transformer (Guo et al., 2019), Sparse Transformer (Child et al., 2019), Longformer (Beltagy et al., 2020) and BigBird (Zaheer et al., 2021). Compared to all those patterns, our proposed Hypercube Transformer adapts a fixed simple sparse pattern and is easy to implement. The recent flat butterfly pattern (Chen et al., 2021) is also another simple sparse pattern with $O(N \log N)$ complexity with input length N. NAS has been applied to learning sparse patterns like SparseBERT (Shi et al., 2021), but searching methods cannot be applied to long-context tasks. Besides, their learned sparse patterns are data-dependent and cannot generalize.

6. Conclusion

We have introduced Normalized Information Payload (NIP), a graph scoring function for various graphs used in Transformer attention mechanism. By taking Computational Complexity and Information Payload into consideration, we can analyze sparse graphs via NIP to find what dense graph do we need for self-attention. After examining existed sparse patterns with NIP, we further present hypercube and utilize it in simple masked-based sparse Transformer. Hypercube Transformer achieves comparable or even better performances compared to strong baselines in pretrain tasks in NLP and long-context sequence modeling while reducing the usage of memory and computation. Experiments on different graphs on LRA benchmark also lay validation for

Table 6. Performances on GLUE test sets. For our implementation, results for RTE, STS and MRPC are reported by first finetuning on the MNLI model instead of the baseline pretrained model.

	MNLI-m/mm	**QNLI**	**QQP**	**RTE**	**SST-2**	**MRPC**	**CoLA**	**STS-B**	**Avg.**	**Speedup**
#metric	Acc	Acc	F1	Acc	Acc	F1	Matthew's corr.	Spearman corr.		
#Examples	393k	105k	364k	2.5k	67k	3.7k	8.5k	7k		
BERT	86.0/85.2	92.6	72.0	78.3	94.5	89.9	60.9	87.5	83.0	1×
BERT_{128}	84.9/84.8	91.1	71.0	76.6	93.1	90.4	58.0	88.3	82.0	1×
CubeBERT_{128}	85.9/85.0	90.8	71.3	77.1	**95.3**	86.4	**61.5**	**87.6**	82.3	1.1×

Normalized Information Payload well. We hope our graph scoring function will reveal important parts behind different sparse patterns. In future work, we may utilize hypercube structure in other modules like MLPs. Another potential direction is to apply Hypercube Transformer to NLP tasks requiring long-context modeling like summarization and question answering.

Acknowledgements

This work was supported by the National Key Research and Development Program of China (No. 2020AAA0108702), the National Natural Science Foundation of China (No. 62022027) and the major key project of PCL (No. PCL2021A12).

References

Beltagy, I., Peters, M. E., and Cohan, A. Longformer: The long-document transformer, 2020.

Chen, B., Dao, T., Liang, K., Yang, J., Song, Z., Rudra, A., and Re, C. Pixelated butterfly: Simple and efficient sparse training for neural network models, 2021.

Child, R., Gray, S., Radford, A., and Sutskever, I. Generating long sequences with sparse transformers, 2019.

Chung, F. and Lu, L. The average distances in random graphs with given expected degrees. *Proceedings of the National Academy of Sciences*, 99(25): 15879–15882, 2002. ISSN 0027-8424. doi: 10.1073/pnas.252631999. URL https://www.pnas.org/content/99/25/15879.

Clark, K., Khandelwal, U., Levy, O., and Manning, C. D. What does bert look at? an analysis of bert's attention, 2019. URL https://arxiv.org/abs/1906.04341.

Cui, B., Li, Y., Chen, M., and Zhang, Z. Fine-tune BERT with sparse self-attention mechanism. In *Proceedings of the 2019 Conference on Empirical Methods in Natural Language Processing and the 9th International Joint Conference on Natural Language Processing (EMNLP-IJCNLP)*, pp. 3548–3553, Hong Kong, China, November 2019. Association for Computational Linguistics. doi: 10.18653/v1/D19-1361. URL https://aclanthology.org/D19-1361.

Devlin, J., Chang, M.-W., Lee, K., and Toutanova, K. Bert: Pre-training of deep bidirectional transformers for language understanding, 2019.

Dosovitskiy, A., Beyer, L., Kolesnikov, A., Weissenborn, D., Zhai, X., Unterthiner, T., Dehghani, M., Minderer, M., Heigold, G., Gelly, S., Uszkoreit, J., and Houlsby, N. An image is worth 16x16 words: Transformers for image recognition at scale, 2021.

Gao, L., Biderman, S., Black, S., Golding, L., Hoppe, T., Foster, C., Phang, J., He, H., Thite, A., Nabeshima, N., Presser, S., and Leahy, C. The pile: An 800gb dataset of diverse text for language modeling, 2020.

Gray, S., Radford, A., and Kingma, D. P. Gpu kernels for block-sparse weights. *arXiv preprint arXiv:1711.09224*, 3:2, 2017.

Guo, M., Ainslie, J., Uthus, D., Ontanon, S., Ni, J., Sung, Y.-H., and Yang, Y. Longt5: Efficient text-to-text transformer for long sequences, 2021.

Guo, Q., Qiu, X., Liu, P., Shao, Y., Xue, X., and Zhang, Z. Star-transformer. In *Proceedings of HLT-NAACL*, pp. 1315–1325, 2019. URL https://www.aclweb.org/anthology/N19-1133.

Ho, J., Kalchbrenner, N., Weissenborn, D., and Salimans, T. Axial attention in multidimensional transformers, 2019.

Hochreiter, S. and Schmidhuber, J. Long short-term memory. *Neural Computation*, 9(8):1735–1780, 1997.

Izsak, P., Berchansky, M., and Levy, O. How to train bert with an academic budget, 2021.

Katzav, E., Biham, O., and Hartmann, A. K. Distribution of shortest path lengths in subcritical erdős-rényi networks. *Physical Review E*, 98(1):012301, 2018.

Lee-Thorp, J., Ainslie, J., Eckstein, I., and Ontanon, S. Fnet: Mixing tokens with fourier transforms, 2021.

Li, X., Liu, S., Chen, H., and Wang, K. A potential information capacity index for link prediction of complex networks based on the cannikin law. *Entropy*, 21 (9), 2019. ISSN 1099-4300. doi: 10.3390/e21090863. URL https://www.mdpi.com/1099-4300/21/9/863.

Lin, T., Wang, Y., Liu, X., and Qiu, X. A survey of transformers, 2021.

Ma, X., Kong, X., Wang, S., Zhou, C., May, J., Ma, H., and Zettlemoyer, L. Luna: Linear unified nested attention, 2021.

Miller, D. Leveraging bert for extractive text summarization on lectures, 2019.

Shi, H., Gao, J., Ren, X., Xu, H., Liang, X., Li, Z., and Kwok, J. T. Sparsebert: Rethinking the importance analysis in self-attention, 2021. URL https://arxiv.org/abs/2102.12871.

Sun, C., Huang, L., and Qiu, X. Utilizing bert for aspect-based sentiment analysis via constructing auxiliary sentence, 2019.

Tay, Y., Dehghani, M., Abnar, S., Shen, Y., Bahri, D., Pham, P., Rao, J., Yang, L., Ruder, S., and Metzler, D. Long range arena: A benchmark for efficient transformers, 2020a.

Tay, Y., Dehghani, M., Bahri, D., and Metzler, D. Efficient transformers: A survey, 2020b.

Tillet, P., Kung, H. T., and Cox, D. *Triton: An Intermediate Language and Compiler for Tiled Neural Network Computations*, pp. 10–19. Association for Computing Machinery, New York, NY, USA, 2019. ISBN 9781450367196. URL https://doi.org/10.1145/3315508.3329973.

Vaswani, A., Shazeer, N., Parmar, N., Uszkoreit, J., Jones, L., Gomez, A. N., Kaiser, L., and Polosukhin, I. Attention is all you need, 2017.

Xiong, Y., Zeng, Z., Chakraborty, R., Tan, M., Fung, G., Li, Y., and Singh, V. Nyströmformer: A nyström-based algorithm for approximating self-attention, 2021.

Yuan, L., Chen, Y., Wang, T., Yu, W., Shi, Y., Jiang, Z., Tay, F. E., Feng, J., and Yan, S. Tokens-to-token vit: Training vision transformers from scratch on imagenet, 2021.

Zaheer, M., Guruganesh, G., Dubey, A., Ainslie, J., Alberti, C., Ontanon, S., Pham, P., Ravula, A., Wang, Q., Yang, L., and Ahmed, A. Big bird: Transformers for longer sequences, 2021.

Zhu, Z. and Soricut, R. H-transformer-1d: Fast one-dimensional hierarchical attention for sequences, 2021.

A. Computation for Normalized Information Payload

Since computation for NIP(G) is related to CC(G) and IP(G), we respectively show these two parts.

A.1. Computation for CC(G)

We compute $\rho(G)$ and $\kappa(G)$ to get CC(G). For all graphs, $\rho(G)$ can be computed easily through definition. For E-R random graph, we choose the probability of every edge to exist p to be $\Theta\left(\frac{\log N}{N}\right)$ for the sake of connectivity. $\kappa(G)$ is the diameter of the graph, which can be straightforwardly computed by definition of graphs. For E-R random graph, the shortest path between any two nodes is logarithmic in the number of nodes (Chung & Lu, 2002; Katzav et al., 2018), thus it equals to $\Theta(\log N)$. For w used in ring lattice, we assume $w \ll N$ for approximation.

$\rho(G)$, $\kappa(G)$ and CC(G) for graphs in Table 1 are listed in Table 7.

Table 7. $\rho(G)$, $\kappa(G)$ and CC(G) for graphs in Table 1, where w is the number of neighbors of a ring lattice.

Type of graph	$\rho(G)$	$\kappa(G)$	CC(G)
Complete	$\Theta(N)$	$\Theta(1)$	$\Theta(N)$
E-R random	$\Theta(\log N)$	$\Theta(\log N)$	$\Theta(\log^2 N)$
Tree	$\Theta(1)$	$\Theta(\log N)$	$\Theta(\log N)$
Star	$\Theta(1)$	$\Theta(1)$	$\Theta(1)$
Ring lattice + E-R random	$\Theta(\log N + w)$	$\Theta(\log N)$	$\Theta(\log N(\log N + w))$
Ring lattice + Star (Longformer)	$\Theta(w)$	$\Theta(1)$	$\Theta(w)$
Ring lattice + Star + E-R random (BigBird)	$\Theta(\log N + w)$	$\Theta(1)$	$\Theta(\log N + w)$
Hypercube	$\Theta(\log N)$	$\Theta(\log N)$	$\Theta(\log^2 N)$

A.2. Computation for IP(G)

To computate IP(G), we first find node pair (a, b) whose distance is the diameter of the graph and calculate Information Payload for that node pair.

$$I_{ab} = \sum_{P_{ab} \in \mathcal{P}_{ab}} R(P_{ab}). \tag{7}$$

For graphs in Table 1, $R(P_{ab})$ is constant for all paths $P_{ab} \in \mathcal{P}_{ab}$. So we can compute IP($G$) as folows, where $|\mathcal{P}_{ab}|$ is the number of paths in $\mathcal{P}_{ab}$,

$$I_{ab} = |\mathcal{P}_{ab}| R(P_{ab}). \tag{8}$$

For **Complete graph, Tree, Star graph, Ring lattice + random, Longformer pattern and BigBird pattern**, the number of paths $|\mathcal{P}_{ab}|$ is 1 and that path can be easily found. $R(P_{ab})$ for that path can be computed by definition. Here we choose the degree of non-global node in Longformer pattern and BigBird pattern to be w and $\log N + w$ respectively.

For **E-R random graph and Ring lattice + E-R random**, we assume adding neighbors does not shorten the diameter of the graph. Thus the $|\mathcal{P}_{ab}|$ and length of the shortest path between any two nodes in ring lattice + E-R random is the same as those in E-R random graph. In E-R random graph, the expected number of a k-length path between two nodes is $p^k(k-1)!C_{N-2}^{k-1}$ where p is the probability for one edge to exist. That is the value of $|\mathcal{P}_{ab}|$. The expected degree for every node in E-R random graph and ring lattice + E-R random is $\Theta(\log N)$ and $\Theta(\log N + w)$ respectively, so the expectation of R for one path is $\Theta(\frac{1}{(\log N)^{\log N}})$ and $\Theta\left(\frac{1}{(\log N + w)^{\log N}}\right)$ respectively. In this case, $k = \log N$ and $p = \Theta(\frac{\log N}{N})$, we

Table 8. Information Payload for one path $R(P_{ab})$ and the number of paths $|\mathcal{P}_{ab}|$ between node a and node b. w is the number of neighbors of a ring lattice. p is the probability of one edge exist in E-R random graph and is set as $\Theta(\frac{\log N}{N})$ for IP(G).

Type of graph	$R(P_{ab})$	$\lvert\mathcal{P}_{ab}\rvert$	IP(G)
Complete	$\Theta\left(\frac{1}{N}\right)$	1	$\Theta\left(\frac{1}{N}\right)$
E-R random	$\Theta\left(\frac{1}{(\log N)^{\log N}}\right)$	$p^k(k-1)!C_{N-2}^{k-1}$	$\Theta\left(\frac{(N-2)!}{N^{\log N}(N-\log N)!}\right)$
Tree	$\Theta(\frac{1}{N^{\log(9)}})$	1	$\Theta(\frac{1}{N^{\log(9)}})$
Star	$\Theta\left(\frac{1}{N}\right)$	1	$\Theta\left(\frac{1}{N}\right)$
Ring lattice + E-R random	$\Theta\left(\frac{1}{(\log N+w)^{\log N}}\right)$	$p^k(k-1)!C_{N-2}^{k-1}$	$\Theta\left(\frac{(N-2)!}{(N+\frac{w}{\log N})^{\log N}(N-\log N)!}\right)$
Ring lattice + Star (Longformer)	$\Theta\left(\frac{1}{Nw}\right)$	1	$\Theta\left(\frac{1}{Nw}\right)$
Ring lattice + Star + E-R random (BigBird)	$\Theta\left(\frac{1}{N(\log N+w)}\right)$	1	$\Theta\left(\frac{1}{N(\log N+w)}\right)$
Hypercube	$\Theta\left(\frac{1}{(\log N)^{\log N}}\right)$	$(\log N)!$	$\Theta\left(\frac{(\log N)!}{(\log N)^{\log N}}\right)$

compute IP(G) for E-R random graph as follows for example.

$$\text{IP}(G) = p^k(k-1)!C_{N-2}^{k-1} \times \Theta\left(\frac{1}{(\log N)^{\log N}}\right) \tag{9}$$

$$= \Theta\left((\frac{\log N}{N})^{\log N}(\log N-1)!C_{N-2}^{\log N-1}\frac{1}{(\log N)^{\log N}}\right) \tag{10}$$

$$= \Theta\left(\frac{(\log N-1)!C_{N-2}^{\log N-1}}{N^{\log N}}\right) \tag{11}$$

$$= \Theta\left(\frac{(N-2)!}{N^{\log N}(N-\log N)!}\right). \tag{12}$$

For **Hypercube**, every node in P_{ab} has a degree of $\Theta(\log N)$ and $len(P_{ab})$ equals to $\Theta(\log N)$, so $R(P_{ab})$ is $\Theta\left(\frac{1}{(\log N)^{\log N}}\right)$. For $|\mathcal{P}_{ab}|$, we consider the choices of every step in the random walk. For the first step it is $\log N$, and it is $\log N - 1$ for the second step. Thus the $|\mathcal{P}_{ab}|$ equals to the full-permutation number of $\log N$, $(\log N)!$.

B. Proofs and Algorithm

B.1. Proof for Theorem 2.4

Theorem 2.4 states that Information Payload between two nodes I_{ab} equals to the probability of a random walk starts from node b that ends in node a at step $len(P_{ab})$.

Proof. First we introduce lemma B.1.

Lemma B.1. *Information Payload for one path $R(P_{ab})$ equals to the probability ($Pr(P_{ba})$) of a random walk starts from b and ends in a following reversed path of P_{ab}.*

Proof. Let us consider random walk on the reversed path of P_{ab}, namely P_{ba}. For the ith step we take, the probability equals to $1/deg(v)$ where v is the node that we are at the $i-1$th step. So the total probability of this path is $Pr(P_{ba}) = \prod_{v\in\mathcal{P}_{ba}\ \&\ v\neq a}\frac{1}{deg(v)}$. We know that $\{v|\in P_{ba}\ \ \&\ \ v\neq a\}$ equals to $\{v|v\in P_{ab}\ \ \&\ \ v\neq a\}$. So $R(P_{ab}) = Pr(P_{ba})$. □

Then, the probability of a random walk starts from b that ends in a at the $len(P_{ab})$ step, denoted by $SPr(P_{ba})$ is the

summation of the probability of all paths in P_{ba}.

$$SPr_{ba} = \sum_{P_{ba} \in \mathcal{P}_{ba}} Pr(P_{ba}). \tag{13}$$

For every $R(P_{ab})$, from lemma B.1 we know that for every $P_{ab} \in \mathcal{P}_{ab}$, $R(P_{ab}) = Pr(P_{ba})$. So the Information Payload between two nodes a, b

$$\begin{aligned} I_{ab} &= \sum_{P_{ab} \in \mathcal{P}_{ab}} R(P_{ab}) && (14)\\ &= \sum_{P_{ab} \in \mathcal{P}_{ab}} Pr(P_{ba}) && (15)\\ &= \sum_{P_{ba} \in \mathcal{P}_{ba}} Pr(P_{ba}) && (16)\\ &= SPr_{ba}. && (17) \end{aligned}$$

□

Since we have Theorem 2.4, we can compute IP(G) via random walk as below.

Computing Information Payload IP(G) via random walk. Using adjacent matrix A_G and diagonal matrix $D = diag(\frac{1}{d_1}, \frac{1}{d_2}, ...\frac{1}{d_N})$, we can easily calculate I_{ab} by random walk.

For each a, b, we have

$$\begin{aligned} M &= DA_G, \\ M^i &= M^{len(P_{ab})}, \\ I_{ab} &= [(M^i)^T]_{ab}. \end{aligned} \tag{18}$$

According to Definition 2.5, let $len(P_{ab}) = \kappa(G)$ in equation (18) and Δ be the set of node pairs whose distance is the diameter of the graph, we can get

$$\text{IP}(G) := \min_{(a,b)\in\Delta}([((DA_G)^{\kappa(G)})^T]_{ab}). \tag{19}$$

B.2. Proof for Theorem 3.1

Theorem 3.1 states that larger block size makes star graph and hypercube have less Normalized Information Payload.

Proof. Given one graph $G_0(\mathcal{V}_0, \mathcal{E}_0)$ where $|\mathcal{V}_0| = N_0$, we denote the two graphs adapting block sparse with different block sizes x and y by $G_x(\mathcal{V}_x, \mathcal{E}_x)$ and $G_y(\mathcal{V}_y, \mathcal{E}_y)$. We know that $|\mathcal{V}_x|$ and $|\mathcal{V}_y|$ all equal to N_0. Let $x < y$, our goal is to prove that NIP(G_x) > NIP(G_y).

We first use b to denote the block size and deduce NIP(G_b). We have another affiliated graph $G_{1/b}(\mathcal{V}_{1/b}, \mathcal{V}_{1/b})$ where $|\mathcal{V}_{1/b}| = \frac{N_0}{b}$ that adapts the same sparse pattern as G_0. Here we use a function of sequence length N to denote NIP(G), namely $NIP_G(N)$.

We first consider CC(G_b).

$$\begin{aligned} \kappa(G_b) &= \kappa(G_{1/b}), && (20)\\ \rho(G_b) &= b\rho(G_{1/b}), && (21)\\ & && (22) \end{aligned}$$

So

$$\text{CC}(G_b) = b \cdot \text{CC}(G_{1/b}). \tag{23}$$

Next, for IP(G_b), the longest path in G_b is equal to that in $G_{1/b}$, while any node v in the path changes its degree $deg(v)$ to $b \cdot deg(v)$. Thus we have

$$\text{IP}(G_b) = \frac{\text{IP}(G_{1/b})}{b^{\kappa(G_{1/b})}}. \tag{24}$$

The final NIP(G_b) then

$$\begin{aligned}
\text{NIP}(G_b) &= \frac{\text{IP}(G_b)}{\text{CC}(G_b)} && (25)\\
&= \frac{\text{IP}(G_{1/b})}{b \cdot \text{CC}(G_{1/b}) b^{\kappa(G_{1/b})}} && (26)\\
&= \frac{1}{b^{\kappa(G_{1/b})+1}} \text{NIP}(G_{1/b}) && (27)\\
&= \frac{1}{b^{\kappa(G_{1/b})+1}} NIP_G\left(\frac{N_0}{b}\right). && (28)
\end{aligned}$$

Let $f(b) = \text{NIP}(G_b)$, our goal is to prove that $f(b)$ is monotonically decreasing for star, hypercube.

Star graph. While $\kappa(G)$ for star is always 2, the $f(b)$ for star is as follows

$$\begin{aligned}
f(b) &= \frac{1}{b^3} NIP_G\left(\frac{N_0}{b}\right) && (29)\\
&= \frac{b}{N_0 b^3} && (30)\\
&= \frac{1}{N_0 b^2}. && (31)
\end{aligned}$$

It's monotonically decreasing for b.

Hypercube. We do the same computation for hypercube. $\kappa(G)$ for hypercube is $\log N$, so

$$\begin{aligned}
f(b) &= \frac{1}{b^{\log N_0+1}} NIP_G\left(\frac{N_0}{b}\right) && (32)\\
&= \frac{1}{b^{\log N_0+1}} \frac{(\log \frac{N_0}{b})!}{(\log \frac{N_0}{b})^{\log \frac{N_0}{b}+2}}. && (33)
\end{aligned}$$

Using Sterling Equation to approximate factorial, where c is $\sqrt{2\pi}$, we get

$$\begin{aligned}
f(b) &\approx \frac{1}{b^{\log N_0+1}} \frac{c(\log \frac{N_0}{b})^{(\log \frac{N_0}{b})+\frac{1}{2}} e^{-(\log \frac{N_0}{b})}}{(\log \frac{N_0}{b})^{\log \frac{N_0}{b}+2}} && (34)\\
&= \frac{1}{b^{\log N_0+1}} \frac{c}{(\log \frac{N_0}{b})^{1.5} e^{(\log \frac{N_0}{b})}} && (35)\\
&= \frac{1}{b^{\log N_0+1}} \frac{c}{(\log \frac{N_0}{b})^{1.5} (\frac{N_0}{b})^{\frac{1}{\ln 2}}} && (36)\\
&= \frac{C}{b^{\log N_0+1-\frac{1}{\ln 2}} (\log \frac{N_0}{b})^{1.5}}. && (37)
\end{aligned}$$

while C is another constant. To make $f(b)$ monotonically decreasing, the derivative of $f(b)$ should be less than zero, which is true when

$$\log N_0 + 1 - \frac{1}{\ln 2} > \frac{3}{2 \ln 2 (\log N_0 - \log b)}. \tag{38}$$

Note that $b \leq \frac{N}{2}$, thus we have to prove

$$\log N_0 + 1 - \frac{1}{\ln 2} > \frac{3}{2 \ln 2}, \tag{39}$$

which is true for $N_0 \geq 128$.

Now we have proved Theorem 3.1.

□

B.3. Iterative mapping algorithm

We demonstrate the iterative binary mapping algorithm here. $<<$ means left logical shift for binary numbers.

Algorithm 1 Binary representation of sequences

Input: sequence $S = (s_0, ..., s_{N-1})$
Output: Binary representation $X^N = X_0 X_1 X_2 ... X_i ... X_{N-1}$
Initialize $X = (0, 1)$
repeat
  $Y = ()$
  for i **in** X **do**
    $Y.append(i << 1)$
  end for
  for i **in** reversed X **do**
    $Y.append(i << 1 + 1)$
  end for
  $X = Y$
until $len(X) >= N$
Output: $X^N = X[: N]$

Final representation

$$X_i^d = \left(\lfloor \frac{i \mod 2^{k-d+1}}{2^{k-d}} \rfloor + \lfloor \frac{i \mod 2^{k-d}}{2^{k-d-1}} \rfloor \right) \mod 2 \tag{40}$$

can be proved by mathematical induction .

Proof.

Base case: For $k = 1$, we know that equation (40) is true.

Inductive step: Assume for $k = n - 1$ equation (40) is true we deduce it for $k = n$. If $d = 0$, we can easily verify that equation (40) is true.

For $d \neq 0$ situations, if $i < 2^{n-1}$, according to algorithm 1, $X_i^d(k = n) = X_i^{d-1}(k = n - 1)$, so

$$X_i^d(k = n) = X_i^{d-1}(k = n - 1) \tag{41}$$

$$= \left(\lfloor \frac{i \mod 2^{n-1-(d-1)+1}}{2^{n-1-(d-1)}} \rfloor + \lfloor \frac{i \mod 2^{n-1-(d-1)}}{2^{n-1-(d-1)-1}} \rfloor \right) \mod 2 \tag{42}$$

$$= \left(\lfloor \frac{i \mod 2^{n-d+1}}{2^{n-d}} \rfloor + \lfloor \frac{i \mod 2^{n-d}}{2^{n-d-1}} \rfloor \right) \mod 2. \tag{43}$$

If $i \geq 2^{n-1}$, $X_i^d(k=n) = X_{2^n-1-i}^d(k=n) = X_{2^n-1-i}^{d-1}(k=n-1)$, so

$$X_i^d(k=n) = X_{2^n-1-i}^{d-1}(k=n-1) \tag{44}$$

$$= \left(\lfloor \frac{(2^n-1-i) \mod 2^{n-1-(d-1)+1}}{2^{n-1-(d-1)}} \rfloor + \lfloor \frac{(2^n-1-i) \mod 2^{n-1-(d-1)}}{2^{n-1-(d-1)-1}} \rfloor \right) \mod 2 \tag{45}$$

$$= \left(\lfloor \frac{(2^n-1-i) \mod 2^{n-d+1}}{2^{n-d}} \rfloor + \lfloor \frac{(2^n-1-i) \mod 2^{n-d}}{2^{n-d-1}} \rfloor \right) \mod 2 \tag{46}$$

$$= \left(\lfloor \frac{i \mod 2^{n-d+1}}{2^{n-d}} \rfloor + \lfloor \frac{i \mod 2^{n-d}}{2^{n-d-1}} \rfloor \right) \mod 2. \tag{47}$$

□

C. Hyper-parameters

C.1. Long Range Arena

We put hyper-parameters for LRA here. We set the embedding hidden size to 64 and the hidden size for attention to be 128. Dropout rate and weight decay is different for each task.

Table 9. Hyper-parameters used for all models we trained on Long Range Arena.

Hyper-parameter	**Our Model**
Batch size	32
Number of Layers	4
Number of Shared Layers	2
Hidden size	64
FFN inner hidden size	128
Attention heads	4
Attention head size	32
Block size	16
Dropout	0.1, 0.2, 0.3
Attention Dropout	0
Learning Rate Decay	Cosine
Weight Decay	0, 0.0001
Optimizer	AdamW
Adam ϵ	1e-6
Adam β_1	0.9
Adam β_2	0.98
Gradient Clipping	0
Prediction Head Pooling	mean

Table 10. Sparsity settings. b is the block size.

Graph	**Global tokens**	**Window length**	**Random tokens**	**Blocks (1K)**	**Blocks (2K)**	**Blocks (4K)**
Star	$1 \times b$	0	0	190	382	766
Ring lattice + E-R random	0	$3 \times b$	$5 \times b$	498	1006	2028
Ring lattice + Star (Longformer)	$1 \times b$	$3 \times b$	0	314	634	1274
Ring lattice + Star + E-R random (BigBird)	$1 \times b$	$3 \times b$	$4 \times b$	546	1119	2274
Hypercube	0	_	_	448	1024	2304

C.2. CubeBERT$_{128}$ Hyper-parameters

We present hyper-parameters for pretraining in Table 11 and downstream tasks in Table 12.

Table 11. Hyper-parameters used for CubeBERT$_{128}$ pretraining.

Hyperparameter	**Our Model**
Number of Layers	24
Hidden size	1024
FFN inner hidden size	4096
Attention heads	16
Attention head size	64
Dropout	0.1
Attention Dropout	0.1
Learning Rate Decay	Linear
Weight Decay	0.01
Optimizer	AdamW
Adam ϵ	1e-6
Adam β_1	0.9
Adam β_2	0.98
Gradient Clipping	0.0
Batch Size	4096
Peak Learning Rate	1e-3
Warmup Proportion	2%
Max Steps	240k

Table 12. Hyper-parameters used for downstream tasks,

Hyper-parameter	**GLUE**	**Wikitext103**
Batch Size	{32,16}	8
Learning Rate	{2e-5, 5e-5}	5e-5
Weight Decay	0.01	0
Max Epochs	5	3
Warmup Steps	50	0